NASA Technical Paper 1469

Stress-Concentration Factors for Finite Orthotropic Laminates With a Circular Hole and Uniaxial Loading

C. S. Hong and John H. Crews, Jr.

MAY 1979

NASA

NASA Technical Paper 1469

Stress-Concentration Factors for Finite Orthotropic Laminates With a Circular Hole and Uniaxial Loading

C. S. Hong and John H. Crews, Jr.
Langley Research Center
Hampton, Virginia

National Aeronautics
and Space Administration

**Scientific and Technical
Information Office**

1979

SUMMARY

Stresses were calculated for finite-width orthotropic laminates with a circular hole and remote uniaxial loading using a two-dimensional finite-element analysis with both uniform stress and uniform displacement boundary conditions. Five different laminates were analyzed: quasi-isotropic $[0^\circ/\pm45^\circ/90^\circ]_s$, 0°, 90°, $[0^\circ/90^\circ]_s$, and $[\pm45^\circ]_s$. Computed results are presented for selected combinations of hole-diameter—sheet-width ratio d/w and length-to-width ratio L/w.

For small L/w values, the stress-concentration factors K_{tn} were significantly different for the uniform stress and uniform displacement boundary conditions. Typically, for the uniform stress condition, the K_{tn} values were much larger than for the infinite-strip reference condition; however, for the uniform displacement condition, they were only slightly smaller than for this reference. For long strips, the differences due to boundary conditions were small.

The results for long strips are also presented as width-correction factors, which relate the maximum stress in finite-width laminates to the corresponding infinite-sheet value. For $d/w \leqq 0.33$, these width-correction factors are nearly equal for all five laminates and may be approximated, with a maximum error of less than 5 percent, by using the quasi-isotropic case. This approximation is expected to apply to most practical laminates, provided L/w is sufficiently large.

INTRODUCTION

The stresses at a fastener hole are typically characterized by using an appropriate elastic stress-concentration factor. For metals, the necessary stress-concentration factors for finite-size, isotropic sheets with holes are usually available from the literature. However, for composites very little is known about stress concentrations for finite-size orthotropic laminates. The purpose of this paper is to explore this general problem area for composites and to present results for a broad range of variables.

The study was based on a two-dimensional finite-element analysis of an orthotropic laminate with a circular hole and uniaxial loading. Five graphite/epoxy laminates which covered a wide range of properties were selected for the analysis; these laminates were quasi-isotropic $[0^\circ/\pm45^\circ/90^\circ]_s$, 0°, 90°, $[0^\circ/90^\circ]_s$, and $[\pm45^\circ]_s$. Finite-element models were developed for a wide range of hole-diameter—sheet-width ratios d/w and length-to-width ratios L/w. These models were then analyzed for each laminate using both uniform stress and uniform displacement boundary conditions at the ends of the model.

Results are presented in terms of stress distributions near the hole and as elastic stress-concentration factors for specific combinations of d/w and L/w for each laminate.

SYMBOLS

d	diameter of hole, m
E_{xx}	Young's modulus in x-direction, MPa
E_{yy}	Young's modulus in y-direction, MPa
G_{xy}	shear modulus, MPa
K_{tg}	gross-section stress-concentration factor, $(\sigma_{\theta\theta})_{max}/S_g$
K_{tn}	net-section stress-concentration factor, $(\sigma_{\theta\theta})_{max}/S_n$
K_∞	infinite-sheet stress-concentration factor, $(\sigma_{\theta\theta})_{max}/S_g$
L	length of sheet, m
R	radius of hole, m
r,θ	polar coordinates, m and deg
S_g	gross-section nominal stress, MPa
S_n	net-section nominal stress, MPa
w	width of sheet, m
x,y	Cartesian coordinates, m
ν_{xy}	Poisson's ratio
$\sigma_{\theta\theta}$	stress component in θ-direction, MPa
$(\sigma_{\theta\theta})_{max}$	maximum $\sigma_{\theta\theta}$, MPa

FINITE-ELEMENT ANALYSIS

Figure 1 shows the general problem analyzed in this study. The range of sheet sizes and configurations was generated by using different combinations of d/w and L/w. Specifically, seven values of d/w were used over the range $0.05 \leq d/w \leq 0.91$, and L/w was taken as 1, 2, and 10.

Throughout this study, the hole radius was assumed to equal unity. Accordingly, the range of d/w represented various sheet widths for a single hole

size, rather than a fixed width with various hole sizes. The results would be the same for either choice of assumptions.

Table I presents the elastic constants for the five laminates analyzed in this study. As previously mentioned, these laminates were selected to cover a broad range of composite properties. The 0° laminate properties (ref. 1) were used with lamination theory to calculate the elastic constants for the other laminates. Although the $[0^\circ/\pm45^\circ/90^\circ]_s$ laminate was called a quasi-isotropic laminate, its calculated elastic constants satisfy all the criteria for isotropy. Consequently, the results for this laminate were compared with isotropic solutions from the literature.

Figure 2 shows the finite-element models. The wide-sheet model shown in figure 2(a) is typical of those analyzed. The hole radius was unaltered and the desired values of d/w and L/w were obtained by removing elements from the model width and length. The narrow-strip model (fig. 2(b)) was the only exception to this procedure. For this case, where $d/w = 0.91$, additional refinement was needed in the narrowest portion of the model. The corresponding model for $L/w = 10$ was generated by adding elements to the model length in figure 2(b).

Two types of elements were used. For the wide-sheet model in figure 2(a), linear-strain (6-node) elements comprised the region near the hole ($3R \times 5R$); uniform-strain (3-node) elements comprised the remainder of the model. The narrow-strip model in figure 2(b) consisted entirely of linear-strain elements. These models were analyzed using the BEND finite-element computer program described in reference 2.

As previously mentioned, two different types of loading were considered. For the first case, uniform x-axis tension was specified as a boundary condition. For the second case, uniform x-direction displacement was the specified boundary condition along the end of the model. The applied load corresponding to this uniform displacement case was calculated by summing nodal forces on the end of the model. For comparison, the computed local (near the hole) stresses for each case were normalized by the corresponding net-section nominal stress.

DISCUSSION OF RESULTS

Results are presented in two formats - as stress distributions near the hole and as stress-concentration factors. The stress distributions are briefly discussed to introduce the stress-concentration factors. As previously mentioned, the laminates, as well as the sheet configurations, were selected to provide a wide range of behavior.

Stress Distributions

Stress distributions are presented for each laminate, using $L/w = 10$ and a range of d/w ratios. For this large L/w value, the sheet was assumed to approximate an infinitely long strip with uniform remote stress.

Figure 3 introduces the stress distributions for the $[0^\circ/\pm45^\circ/90^\circ]_s$ quasi-isotropic laminate. Figure 3(a) shows $\sigma_{\theta\theta}$ stresses along the hole boundary and figure 3(b) shows this stress along the y-axis ($\theta = 90^\circ$). The $\sigma_{\theta\theta}$ stresses were normalized by the net-section nominal stress S_n. For simplicity, these figures show results for only three nonzero d/w values. In figures 3(a) and 3(b), the dashed curves represent the infinite-sheet solution where d/w = 0 (ref. 3). Figure 3(a) also shows the stress-concentration factor K_∞ for the infinite-sheet case.

Figure 4 presents results for the 0° laminate. These stress distributions have larger maximum values $(\sigma_{\theta\theta})_{max}$ and larger gradients than in the quasi-isotropic case. (Compare figs. 3 and 4.) These differences are probably caused by the large ratio of longitudinal-to-shear stiffnesses for the 0° laminate. (See table I.) Again, the infinite-sheet results (dashed curves) were calculated using equations from reference 3 and the material properties from table I.

The stress distributions for the 90° laminate are plotted in figure 5. In contrast to the previous two cases, the largest stress magnitude is associated with the compressive stress at $\theta = 0^\circ$, rather than the tensile stress at $\theta = 90^\circ$. As expected, the $[0^\circ/90^\circ]_s$ results in figure 6 are approximately equal to the averages of those shown for the 0° and 90° cases.

The stress distributions for the $[\pm45^\circ]_s$ laminate have some unusual features. Figure 7(a) shows that $(\sigma_{\theta\theta})_{max}$ occurs near $\theta = 60^\circ$ for $d/w \leq 0.5$, rather than at the usual location on the transverse axis ($\theta = 90^\circ$). Also, the location for this peak stress depends on the d/w ratio. Furthermore, figure 7(b) shows that the $\sigma_{\theta\theta}$ away from the hole may be slightly larger than at the hole boundary (r/R = 1.0).

Stress-Concentration Factors

Figure 8 shows results for the quasi-isotropic laminate; net-section stress-concentration factors K_{tn} are plotted against d/w for L/w = 10. For comparison, this figure also includes results from the literature on isotropic strips with a circular hole and uniform stress (refs. 4 and 5). Present results and those from the literature agree closely over the range of finite widths. Furthermore, the curve drawn through these results appears to agree with $K_\infty = 3$.

Figure 9 presents all the K_{tn} results for the quasi-isotropic laminate. For each L/w value, two curves are plotted - one for the uniform stress boundary condition and one for the uniform displacement boundary condition. Results for the stress boundary condition were much more sensitive to L/w than were the uniform displacement results. Below L/w = 2, the stress boundary condition resulted in K_{tn} values much higher than the uniform displacement results; at $L/w \geq 2$, the results were about the same. Numerical results are given in table II.

The K_{tn} results for the 0° laminate are presented in figure 10 and table III. For L/w = 10, stress and displacement boundary conditions

produced the same K_{tn} values. Therefore, the $L/w = 10$ curve is a good approximation to the infinite-strip case, as assumed previously. The curves for $L/w = 1$ and 2 lie above or below this infinite-strip curve, depending on whether the sheet is loaded by the stress or displacement boundary condition. The differences between these curves are much larger than those shown previously for the quasi-isotropic laminate.

The 0° laminate was also used to verify the finite-element procedures. This case was believed to be the most severe of those considered because it had the largest stress gradients. The results for the $L/w = 10$, $d/w = 0.05$ case were compared with the infinite-sheet stress-concentration factor, $K_\infty = 6.430$, from reference 3. For this comparison, the computed K_{tn} was converted to gross-section stress-concentration factor K_{tg}. The uniform displacement and uniform stress conditions yielded K_{tg} values of 6.471 and 6.517, respectively, only 0.6 percent and 1.3 percent larger than K_∞.

Figure 11 and table IV show results for the 90° laminate. For this extreme case, the K_{tn} values are smaller than for the two previous laminates. Also, the curves for different L/w values are rather closely grouped. This indicates a weak L/w influence, which was attributed to the low extensional modulus for the 90° laminate.

The results for the $[0^\circ/90^\circ]_s$ laminate are presented in figure 12 and table V. The L/w influence in figure 12 is larger than for the isotropic case but, as expected, it is intermediate to the extreme behavior displayed by the 0° and 90° laminates. The K_{tn} values for the $[0^\circ/90^\circ]_s$ laminate are nearly averages of those for the 0° and 90° laminates.

The K_{tn} values for the $[\pm 45^\circ]_s$ laminate, presented in figure 13 and table VI, differ somewhat from previous results. For $d/w \leq 0.50$, the K_{tn} results of figure 13 are based on values of $(\sigma_{\theta\theta})_{max}$ located near $\theta = 60^\circ$ on the hole boundary. These K_{tn} values are shown by solid symbols. For very narrow strips ($d/w > 0.50$), the computed K_{tn} values are based on the usual location of $\theta = 90^\circ$ for $(\sigma_{\theta\theta})_{max}$. Note that even for $L/w = 1$, the curve for the uniform displacement case is quite close to the infinite-strip ($L/w = 10$) case, in contrast to the behavior for the uniform stress case. Therefore, the uniform displacement case provides the better approximation to the infinite-sheet case. This conclusion also applies to the other laminates analyzed.

Figure 14 is a comparison of the infinite-strip curves for the five laminates. For $d/w = 0$, the K_{tn} values range from 2.48 to 6.43, compared with 3.0 for the quasi-isotropic laminate. However, for $d/w = 1$, all five extrapolated curves converge to a narrow range of about 1.9 to 2.3. Comparison of the 0° and 90° curves shows that the d/w influence on K_{tn} is quite different for the two laminates. The 0° curve has K_{tn} values from 6.43 to 2.3, a range larger than 60 percent of the maximum K_{tn}. In contrast, d/w has less influence for the 90° laminate; its K_{tn} curve shows K_{tn} from 2.48 to 1.9, a range of only about 20 percent of maximum.

To show how d/w influences $(\sigma_{\theta\theta})_{max}$, the results from figure 14 were replotted in figure 15. For comparison, the values of $(\sigma_{\theta\theta})_{max}$ in this

figure were normalized by corresponding infinite-sheet values of maximum stress $S_g K_\infty$ for each laminate. Therefore, the curves in figure 15 can be interpreted as width corrections which relate the finite-width $(\sigma_{\theta\theta})_{max}$ values to the corresponding infinite-sheet values.

In figure 15, all five curves emanate from $(\sigma_{\theta\theta})_{max}/S_g K_\infty = 1$ and diverge for larger values of d/w. However, these curves diverge gradually, despite the wide range of orthotropic laminate properties that they represent. Surprisingly, for d/w of less than 0.33, all five curves could be approximated by the isotropic curve, with a maximum error of less than 5 percent. This is believed to be significant because the present range of laminate properties and the range $d/w \leqq 0.33$ are expected to cover most practical cases.

CONCLUDING REMARKS

Stresses were calculated for finite-width orthotropic composite sheets with a circular hole and remote uniaxial loading using a two-dimensional finite-element analysis. Five different laminates were analyzed: quasi-isotropic $[0^\circ/\pm45^\circ/90^\circ]_s$, 0°, 90°, $[0^\circ/90^\circ]_s$, and $[\pm45^\circ]_s$. The effects of sheet width and length and the differences between uniform stress and uniform displacement boundary conditions were studied. Stress-concentration factors are presented for various combinations of hole-diameter—sheet-width ratio d/w and length-to-width ratio, L/w.

For small values of L/w, uniform stress and uniform displacement boundary conditions produced significantly different stress-concentration factors, especially for the 0° laminate. Typically, results for the uniform stress boundary condition were much larger than for the infinite-strip reference case; in contrast, for uniform applied displacement the results were only slightly smaller than this reference. For large L/w values, differences due to boundary conditions were small.

Anisotropy had a strong influence on the stress-concentration factors for long strips with small d/w values. At d/w = 0, the K_{tn} values ranged from 6.43 for the 0° laminate to 2.48 for the 90° laminate, compared with 3.0 for the quasi-isotropic $[0^\circ/\pm45^\circ/90^\circ]_s$ laminate. By contrast, for d/w = 1, all extrapolated K_{tn} curves converged to a narrow range of about 1.9 to 2.3.

The results for long strips were also presented as width-correction factors, relating the maximum stress in finite-width laminates to its corresponding infinite-sheet value. For $d/w \leqq 0.33$, these width-correction factors were nearly equal for all five laminates and may be approximated by using the quasi-isotropic case, with a maximum error of less than 5 percent. This approximation is expected to apply to most practical laminates, provided L/w is sufficiently large.

Langley Research Center
National Aeronautics and Space Administration
Hampton, VA 23665
April 18, 1979

REFERENCES

1. Advanced Composites Design Guide. Volume I - Design. Third Edition (Second Revision). Contract No. F33615-74-C-5075, Flight Dyn. Lab., U.S. Air Force, Sept. 1976. (Available from DDC as AD B027 146.)

2. Pifko, A.; Levine, H. S.; and Armen, H., Jr.: PLANS - A Finite Element Program for Nonlinear Analysis of Structures. Volume I - Theoretical Manual. NASA CR-2568, 1975.

3. Lekhnitskii, S. G.: Theory of Elasticity of an Anisotropic Elastic Body. Holden-Day, Inc. (San Francisco), 1963.

4. Howland, R. C. J.: On the Stresses in the Neighbourhood of a Circular Hole in a Strip Under Tension. Philos. Trans. R. Soc. London, ser. A, vol. 229, Jan. 6, 1930, pp. 49-86.

5. Koiter, W. T.: An Elementary Solution of Two Stress Concentration Problems in the Neighbourhood of a Hole. Appl. Math., vol. XV, no. 3, Oct. 1957, pp. 303-308.

TABLE I.- LAMINATE CONSTANTS

Laminate	Elastic constants			
	E_{xx}, MPa	E_{yy}, MPa	G_{xy}, MPa	ν_{xy}
Quasi-isotropic $[0^o/\pm45^o/90^o]_s$	57 890	57 890	22 090	0.310
0^o	146 900	10 890	6 412	0.380
90^o	10 890	146 900	6 412	0.028
$[0^o/90^o]_s$	79 500	79 500	6 412	0.052
$[\pm45^o]_s$	22 250	22 250	37 770	0.735

TABLE II.- STRESS-CONCENTRATION FACTORS FOR THE QUASI-ISOTROPIC LAMINATE

L/w	Loading (a)	Diameter-to-width ratio, d/w						
		0.05	0.10	0.20	0.33	0.50	0.67	0.91
1	S	2.865	2.770	2.676	2.759	3.199	4.451	-----
	D	2.850	2.714	2.468	2.219	2.008	1.916	-----
2	S	2.854	2.729	2.520	2.332	2.193	2.134	2.052
	D	2.854	2.728	2.517	2.328	2.183	2.117	2.040
10	S	-----	-----	2.516	2.326	2.180	2.114	2.040
	D	-----	-----	2.516	2.326	2.180	2.114	2.040

[a]S denotes uniform stress boundary condition; D denotes uniform displacement boundary condition.

TABLE III.- STRESS-CONCENTRATION FACTORS FOR THE 0° LAMINATE

L/w	Loading (a)	Diameter-to-width ratio, d/w						
		0.05	0.10	0.20	0.33	0.50	0.67	0.91
1	S	6.281	6.283	6.623	7.215	8.190	10.598	-----
	D	6.042	5.462	4.384	3.493	2.907	2.667	-----
2	S	6.191	5.967	5.642	5.422	5.102	4.638	3.06
	D	6.147	5.804	5.111	4.360	3.648	3.179	2.538
10	S	-----	-----	5.322	-----	4.054	3.480	2.609
	D	-----	-----	5.322	-----	4.054	3.480	2.609

[a]S denotes uniform stress boundary condition; D denotes uniform displacement boundary condition.

TABLE IV.- STRESS-CONCENTRATION FACTORS FOR THE 90° LAMINATE

L/w	Loading (a)	Diameter-to-width ratio, d/w						
		0.05	0.10	0.20	0.33	0.50	0.67	0.91
1	S	2.358	2.265	2.130	2.088	2.138	2.375	-----
	D	2.355	2.255	2.096	1.980	1.889	1.866	-----
2	S	2.356	2.258	2.109	2.016	1.959	1.959	1.989
	D	2.356	2.258	2.109	2.016	1.959	1.959	1.987
10	S	-----	-----	2.109	-----	1.959	1.959	1.988
	D	-----	-----	2.109	-----	1.959	1.959	1.988

[a]S denotes uniform stress boundary condition; D denotes uniform displacement boundary condition.

TABLE V.- STRESS-CONCENTRATION FACTORS FOR THE $[0^{\circ}/90^{\circ}]_s$ LAMINATE

L/w	Loading (a)	Diameter-to-width ratio, d/w						
		0.05	0.10	0.20	0.33	0.50	0.67	0.91
1	S	4.626	4.516	4.468	4.582	4.939	6.072	-----
	D	4.544	4.224	3.592	2.978	2.540	2.305	-----
2	S	4.592	4.394	4.061	3.738	3.367	3.014	2.400
	D	4.582	4.356	3.933	3.480	3.032	2.719	2.313
10	S	-----	-----	3.991	-----	3.165	2.826	2.340
	D	-----	-----	3.991	-----	3.165	2.826	2.340

[a]S denotes uniform stress boundary condition; D denotes uniform displacement boundary condition.

TABLE VI.- STRESS-CONCENTRATION FACTORS FOR THE $[\pm 45^{\circ}]_s$ LAMINATE

L/w	Loading (a)	Diameter-to-width ratio, d/w						
		0.05 (b)	0.10 (b)	0.20 (b)	0.33 (b)	0.50 (c)	0.67	0.91
1	S	2.745	2.657	2.567	2.628	2.920	3.723	-----
	D	2.741	2.639	2.480	2.295	1.899	1.717	-----
2	S	2.738	2.630	2.457	2.250	1.916	1.772	1.895
	D	2.738	2.630	2.454	2.238	1.904	1.767	1.895
10	S	-----	-----	2.456	-----	1.909	1.766	1.890
	D	-----	-----	2.456	-----	1.909	1.766	1.890

[a]S denotes uniform stress boundary condition; D denotes uniform displacement boundary condition.

[b]$(\sigma_{\theta\theta})_{max}$ occurred at $\theta = 57^{\circ}$.

[c]$(\sigma_{\theta\theta})_{max}$ occurred at $\theta = 63^{\circ}$.

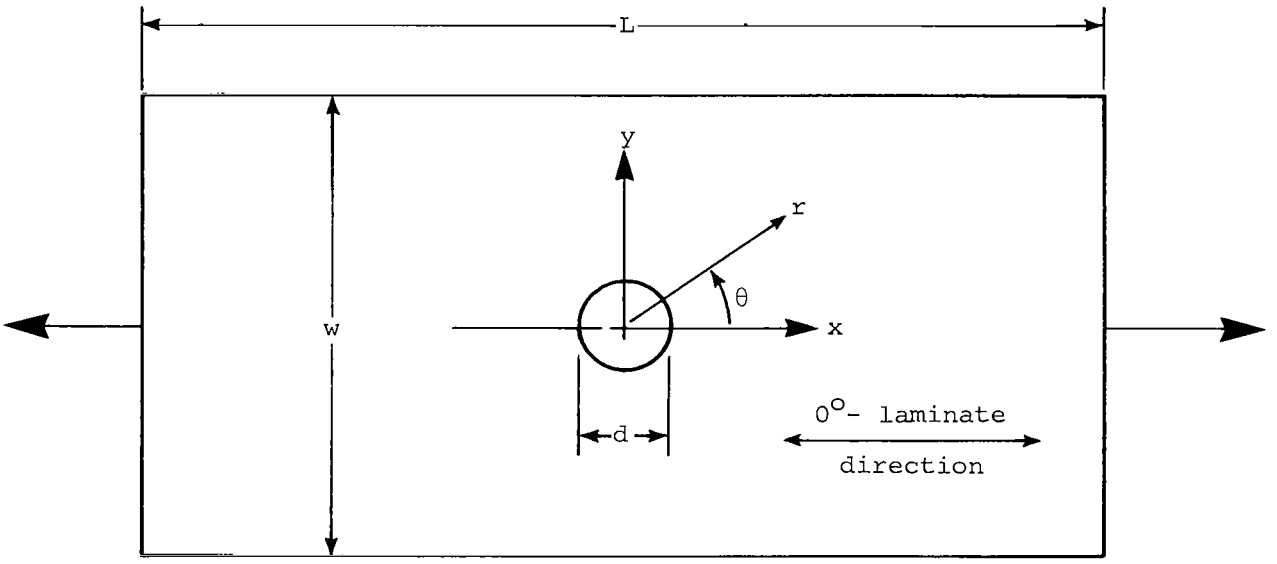

Figure 1.- Sheet configuration and loading.

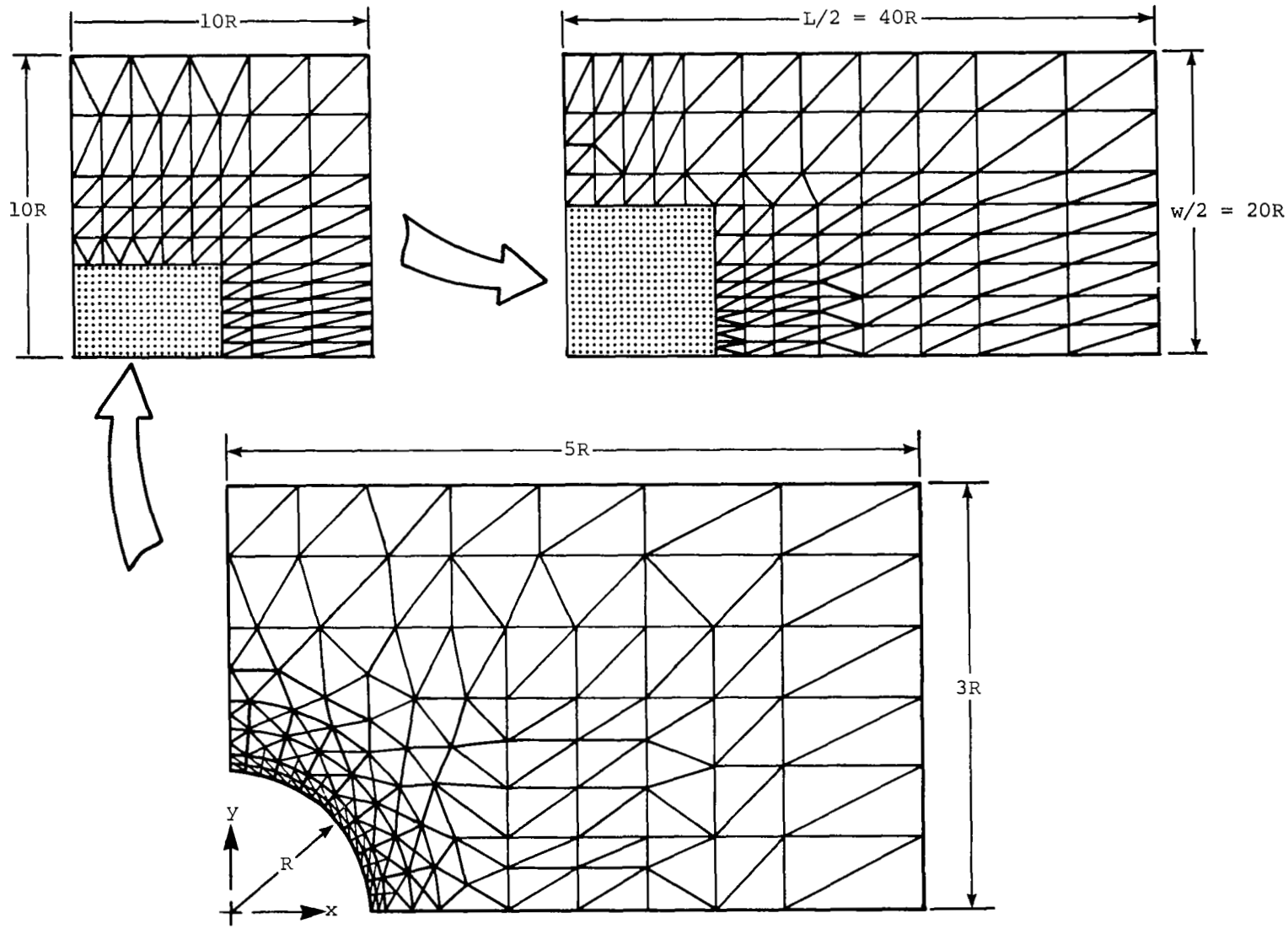

(a) Wide-sheet model.

Figure 2.- Finite-element models.

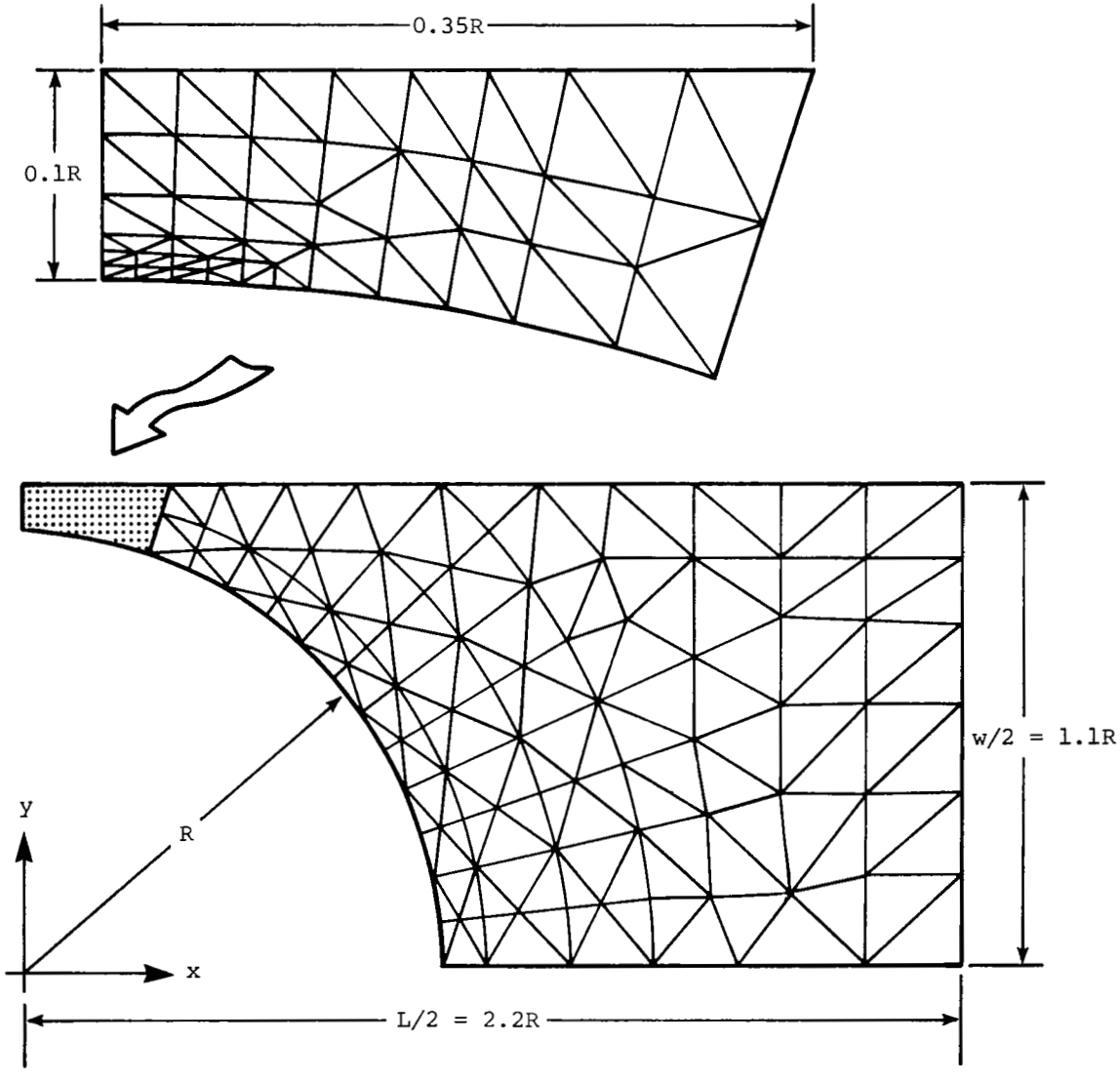

(b) Narrow-strip model.

Figure 2.- Concluded.

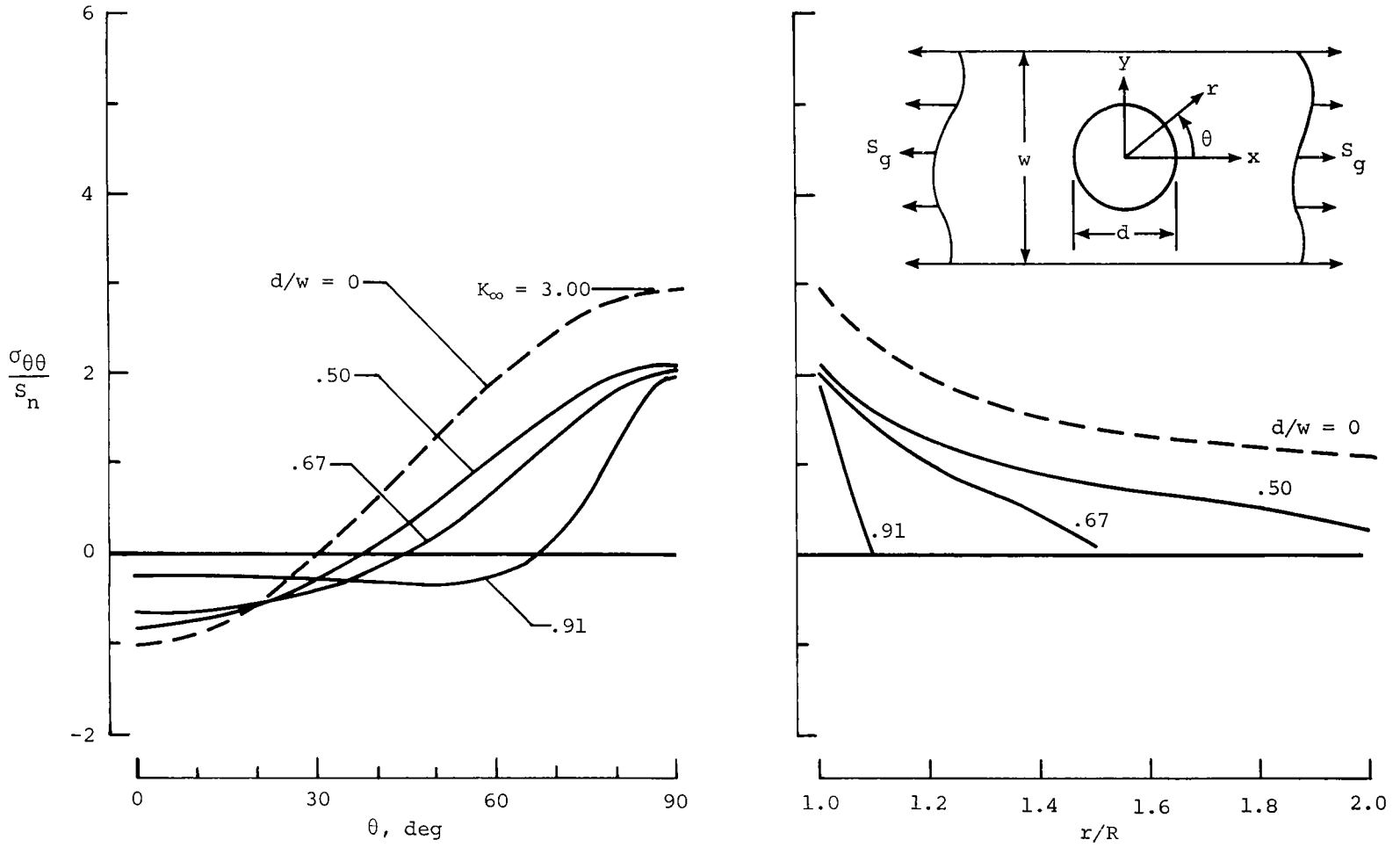

(a) Stress along hole boundary.

(b) Stress along y-axis ($\theta = 90^o$).

Figure 3.- Stresses in quasi-isotropic laminate with uniform stress boundary conditions; L/w = 10.

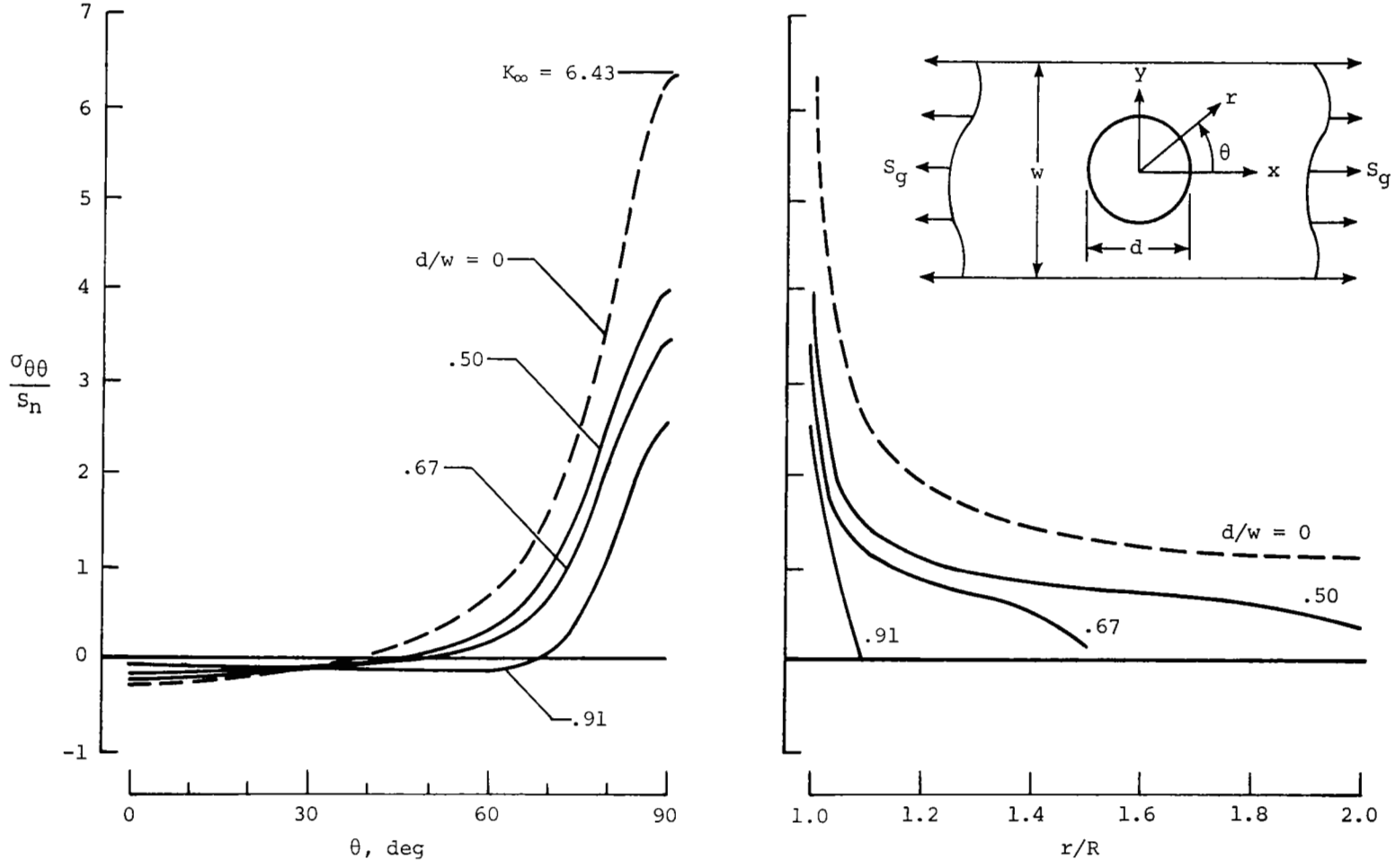

(a) Stress along hole boundary.

(b) Stress along y-axis ($\theta = 90^o$).

Figure 4.- Stresses in 0^o laminate with uniform stress boundary condition; L/w = 10.

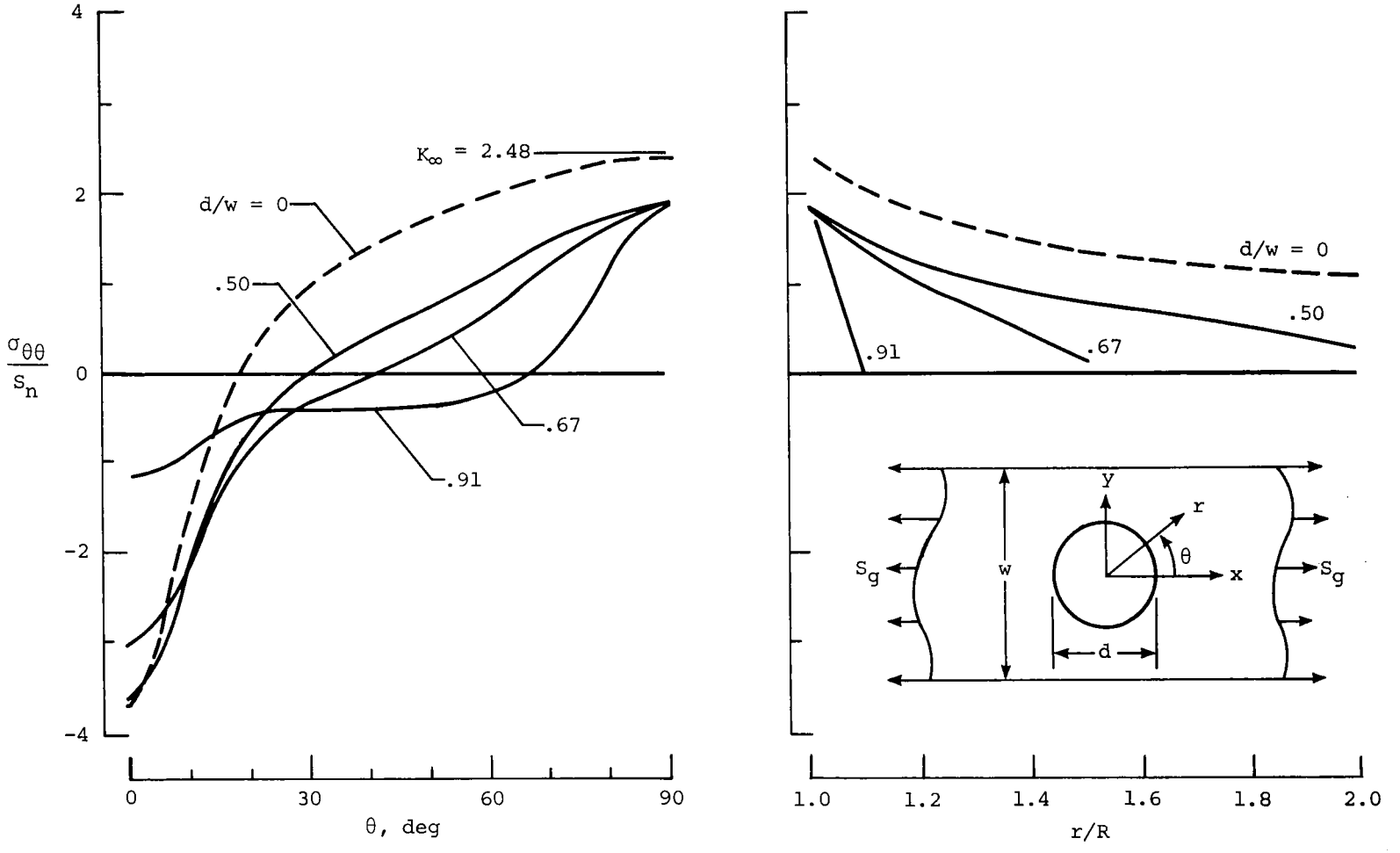

(a) Stress along hole boundary.

(b) Stress along y-axis ($\theta = 90^o$).

Figure 5.- Stresses in 90^o laminate with uniform stress boundary condition; L/w = 10.

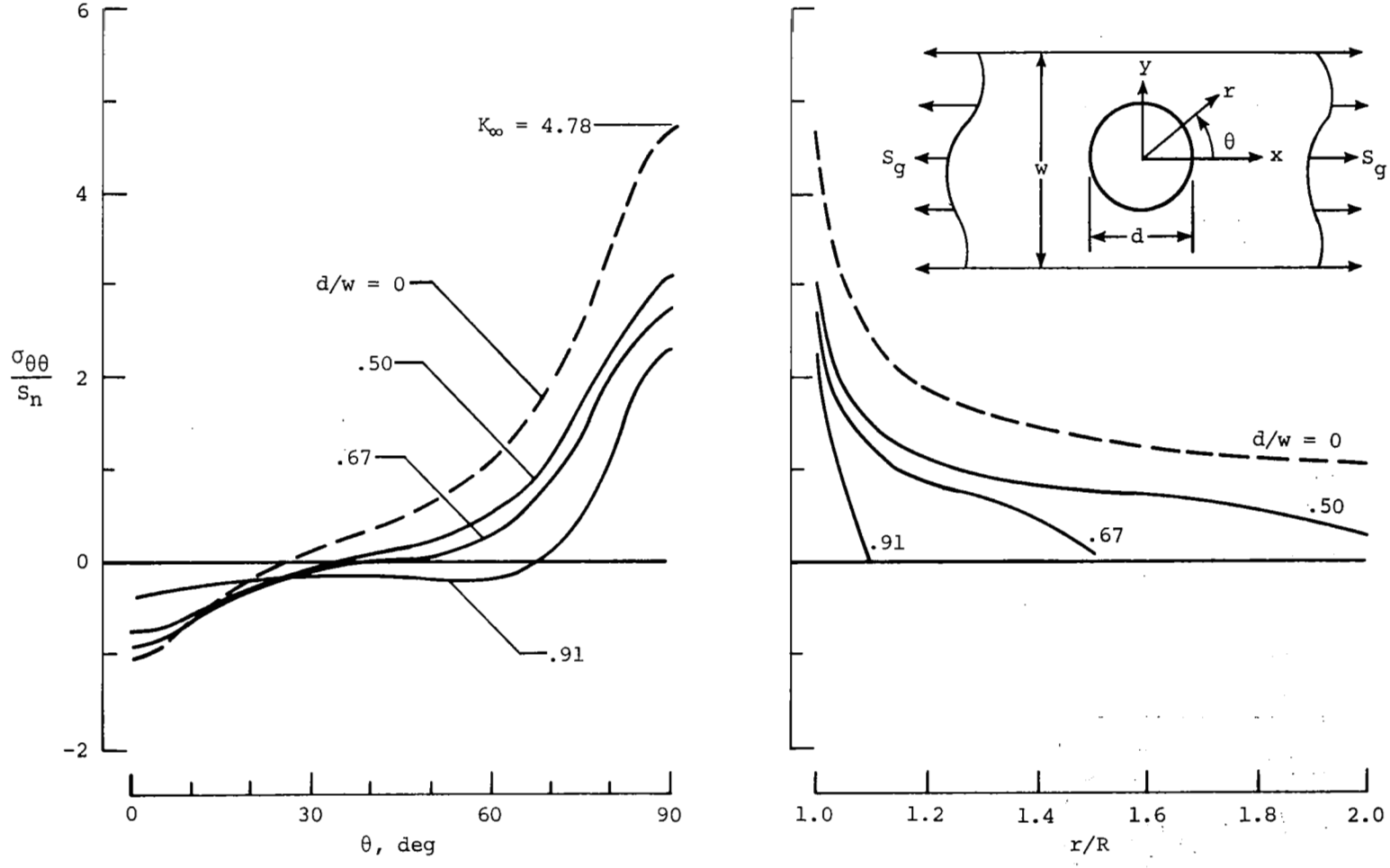

(a) Stress along hole boundary.

(b) Stress along y-axis ($\theta = 90^o$).

Figure 6.- Stresses in $[0^o/90^o]_s$ laminate with uniform stress boundary condition; L/w = 10.

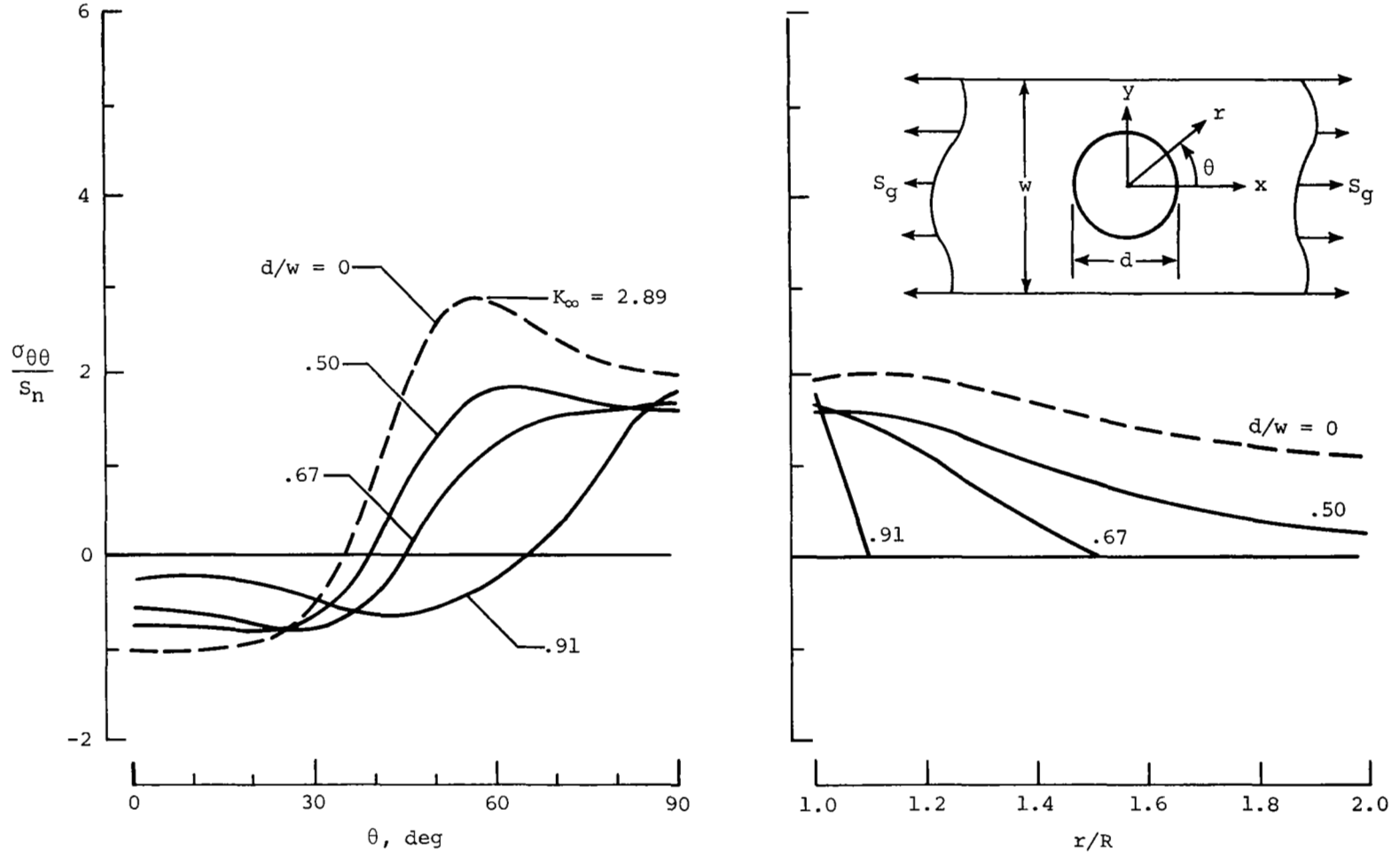

(a) Stress along hole boundary.

(b) Stress along y-axis ($\theta = 90^o$).

Figure 7.- Stresses in $[\pm 45^o]_s$ laminate with uniform stress boundary condition; L/w = 10.

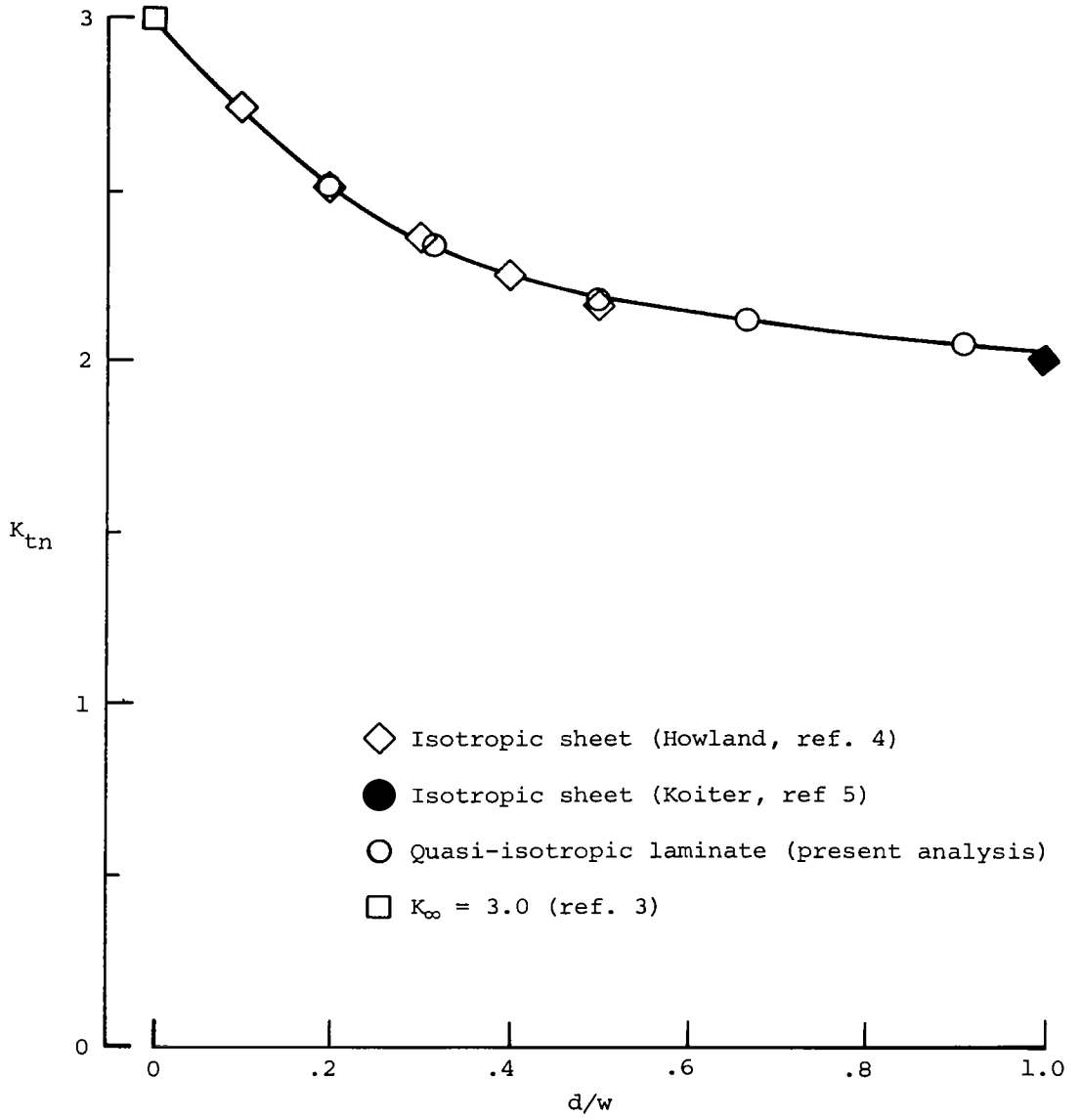

Figure 8.- Stress-concentration factors for a quasi-isotropic laminate with a circular hole and uniform stress boundary condition; L/w = 10.

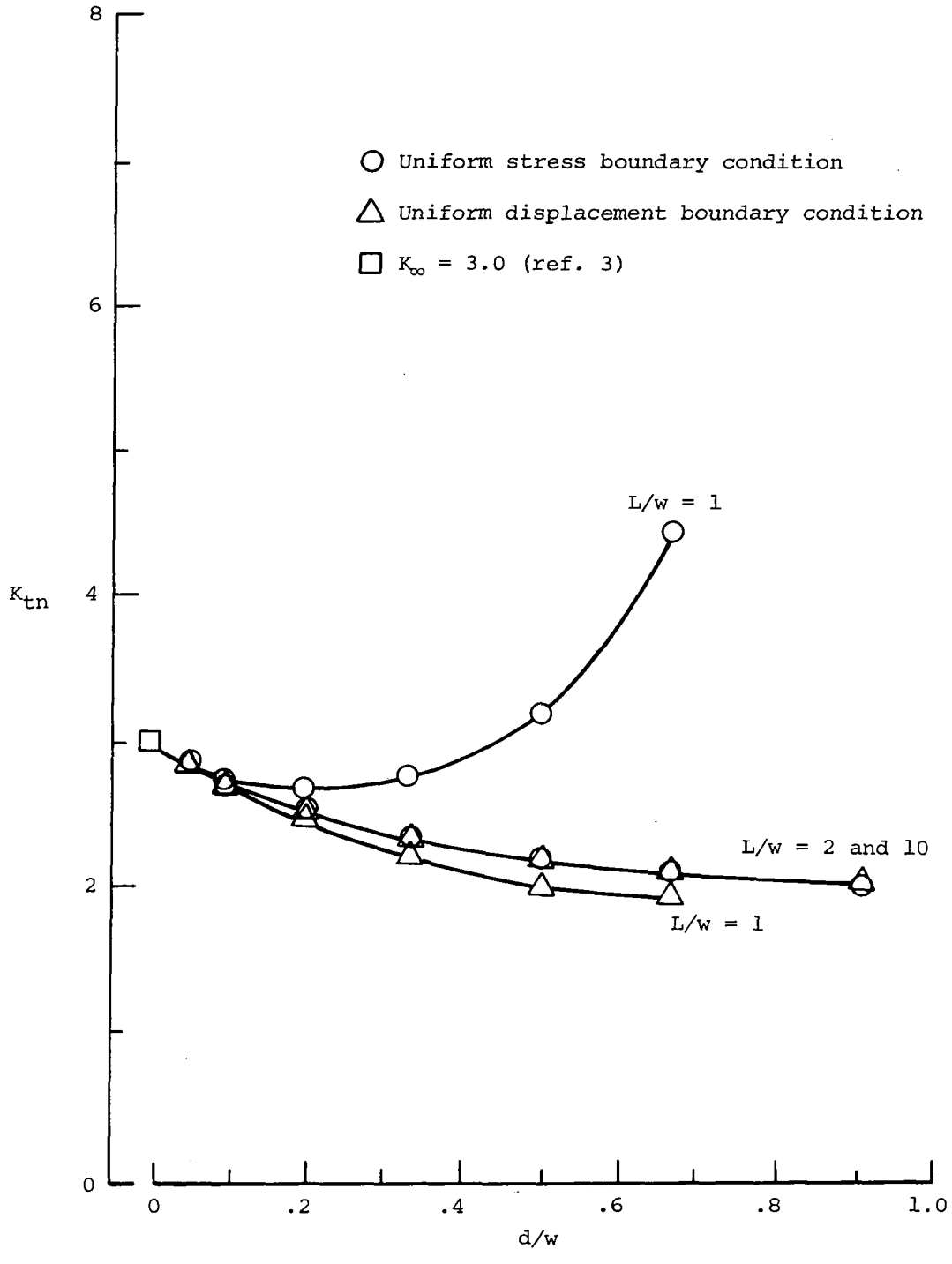

Figure 9.- Stress-concentration factors for a quasi-isotropic laminate with a circular hole.

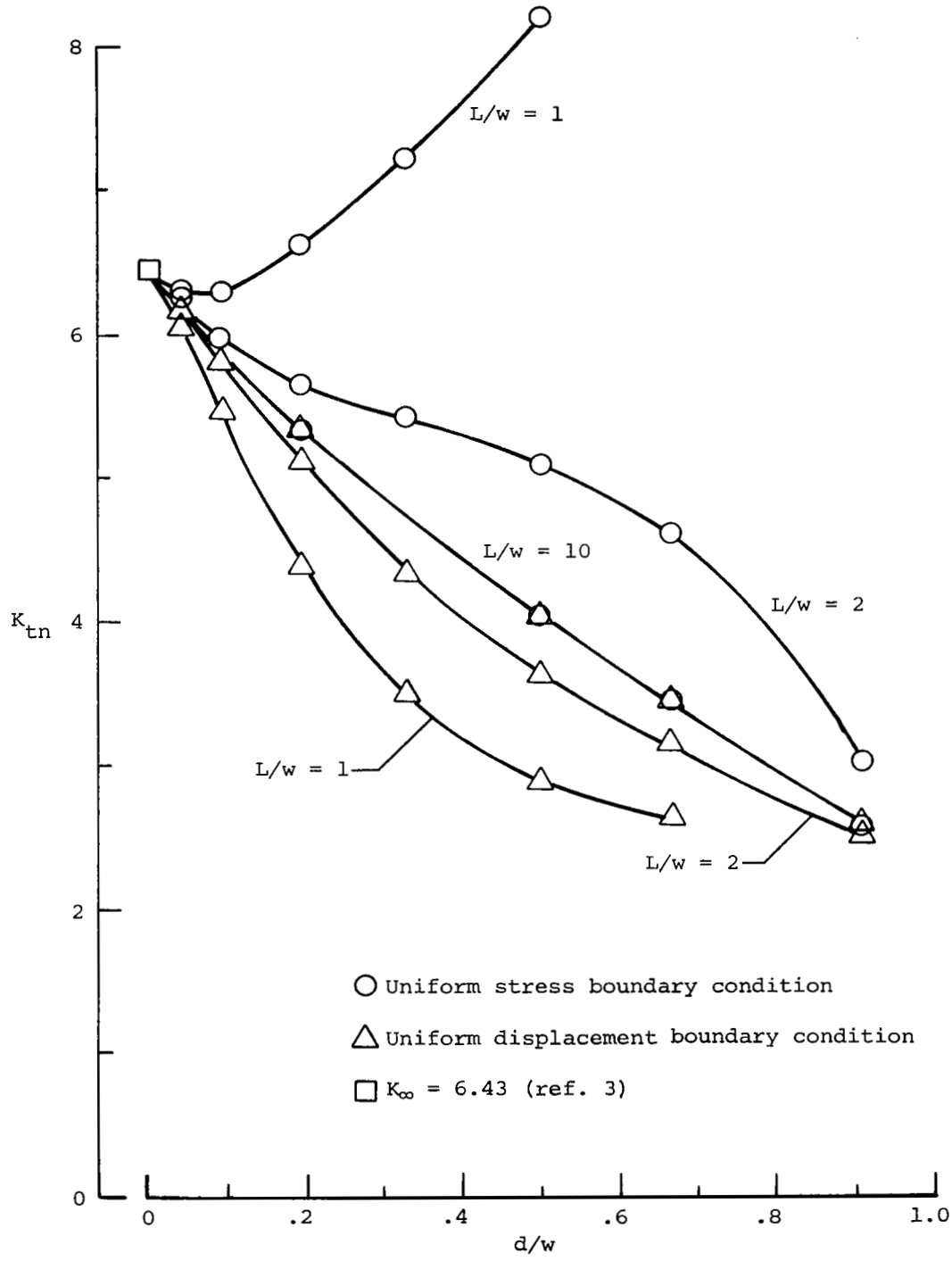

Figure 10.- Stress-concentration factors for a 0° laminate with a circular hole.

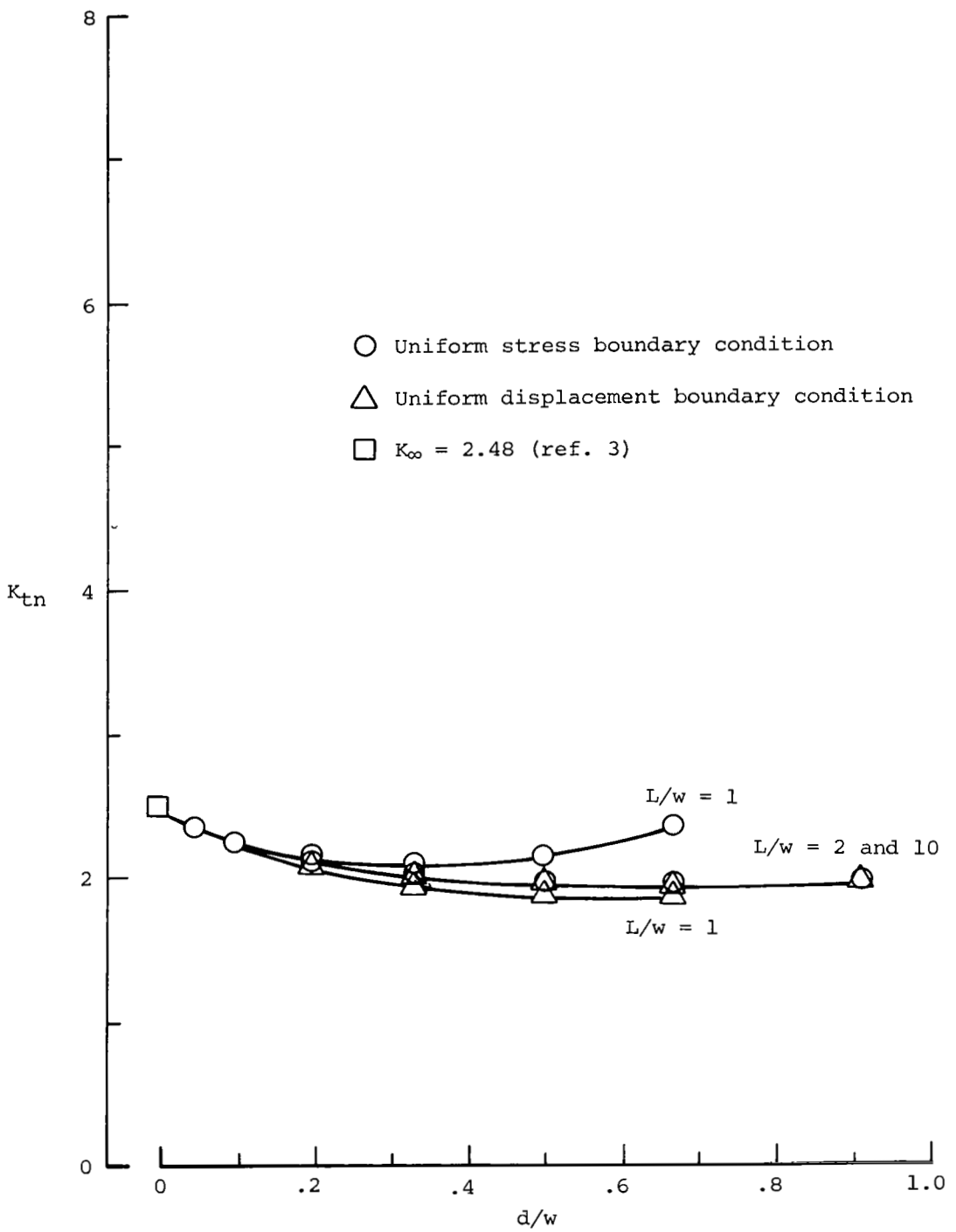

Figure 11.- Stress-concentration factors for a 90° laminate with a circular hole.

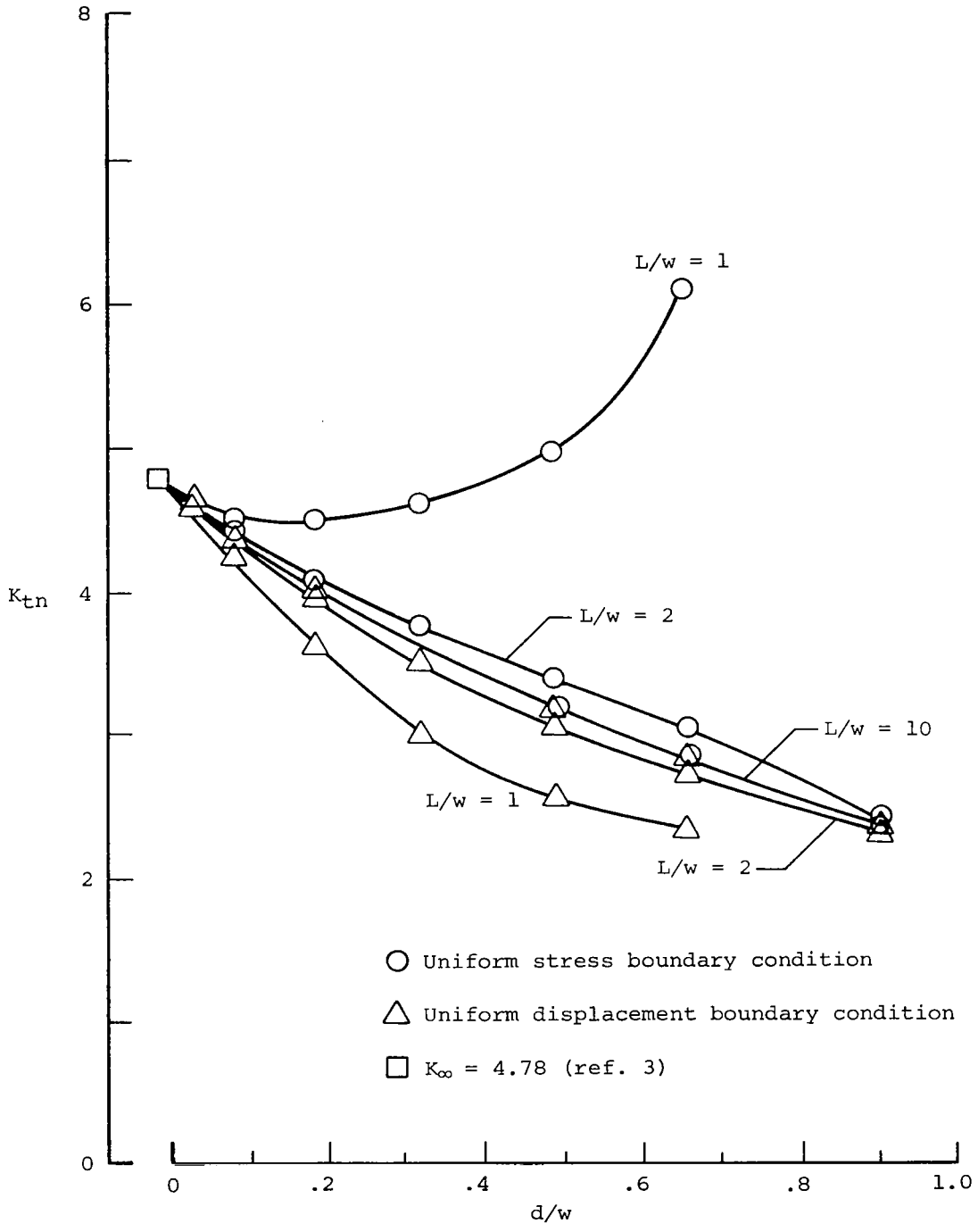

Figure 12.- Stress-concentration factors for a $[0^o/90^o]_s$ laminate with a circular hole.

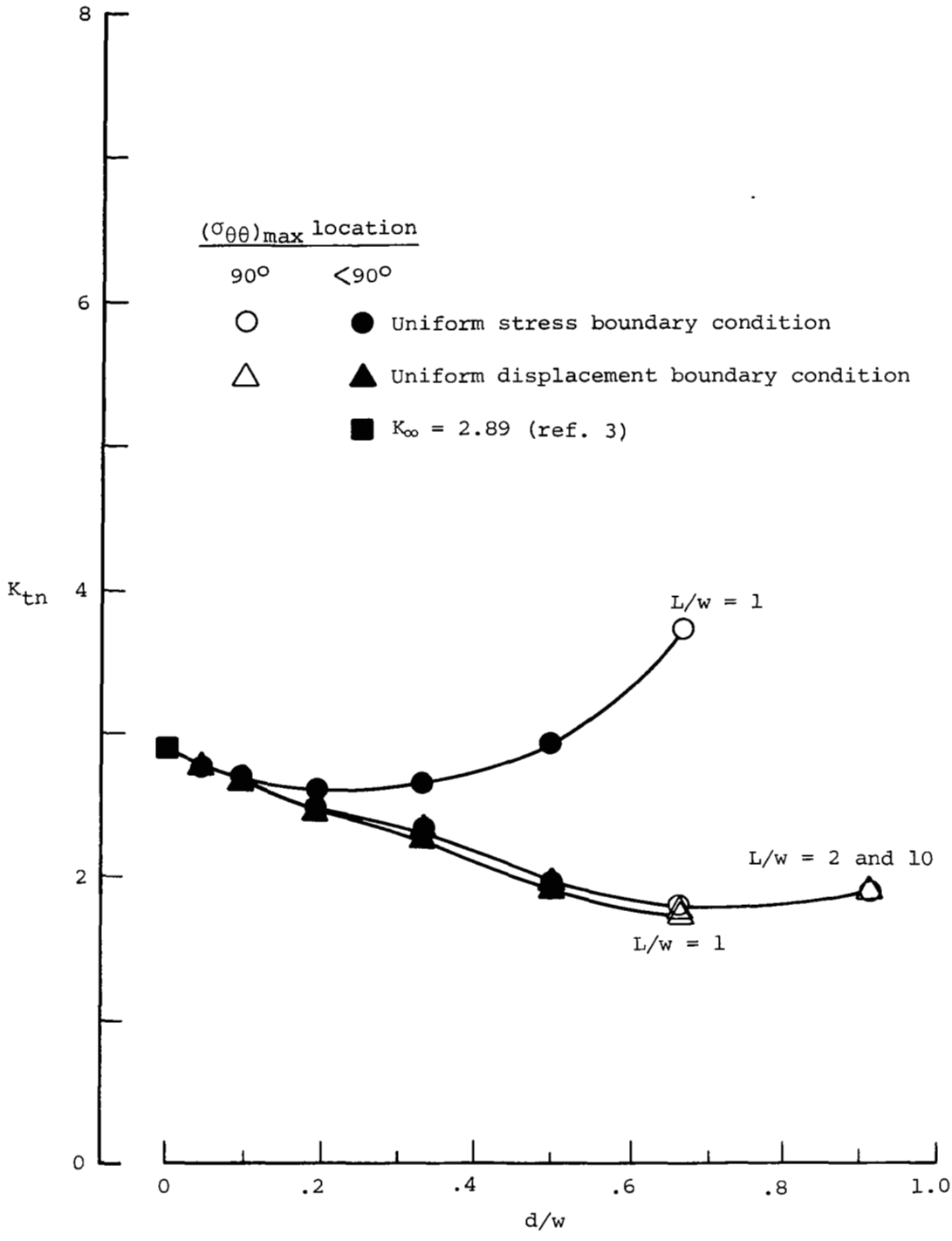

Figure 13.- Stress-concentration factors for a $[\pm 45^o]_s$ laminate with a circular hole.

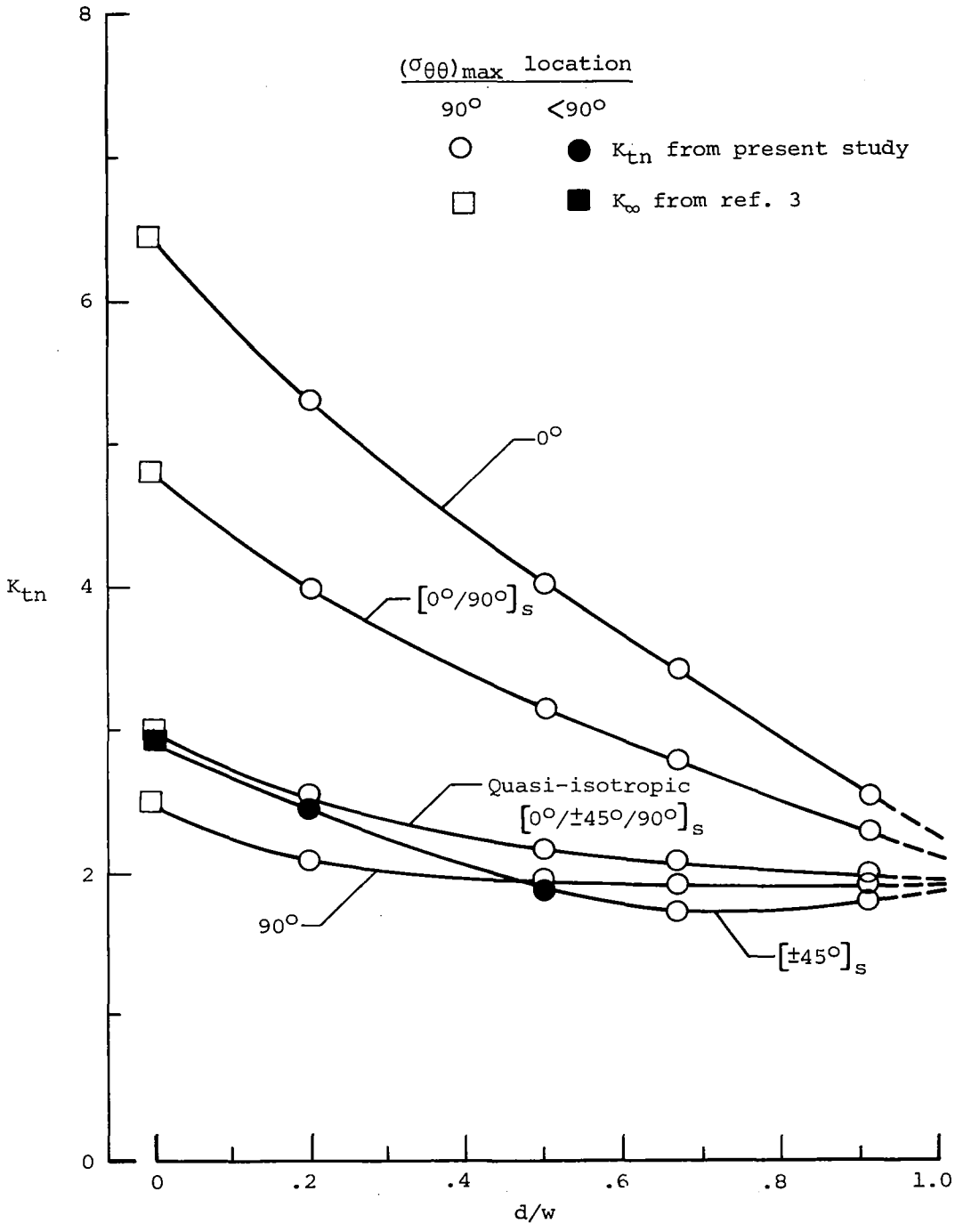

Figure 14.- Stress-concentration factors for orthotropic laminates with a circular hole and uniform stress boundary condition; L/w = 10.

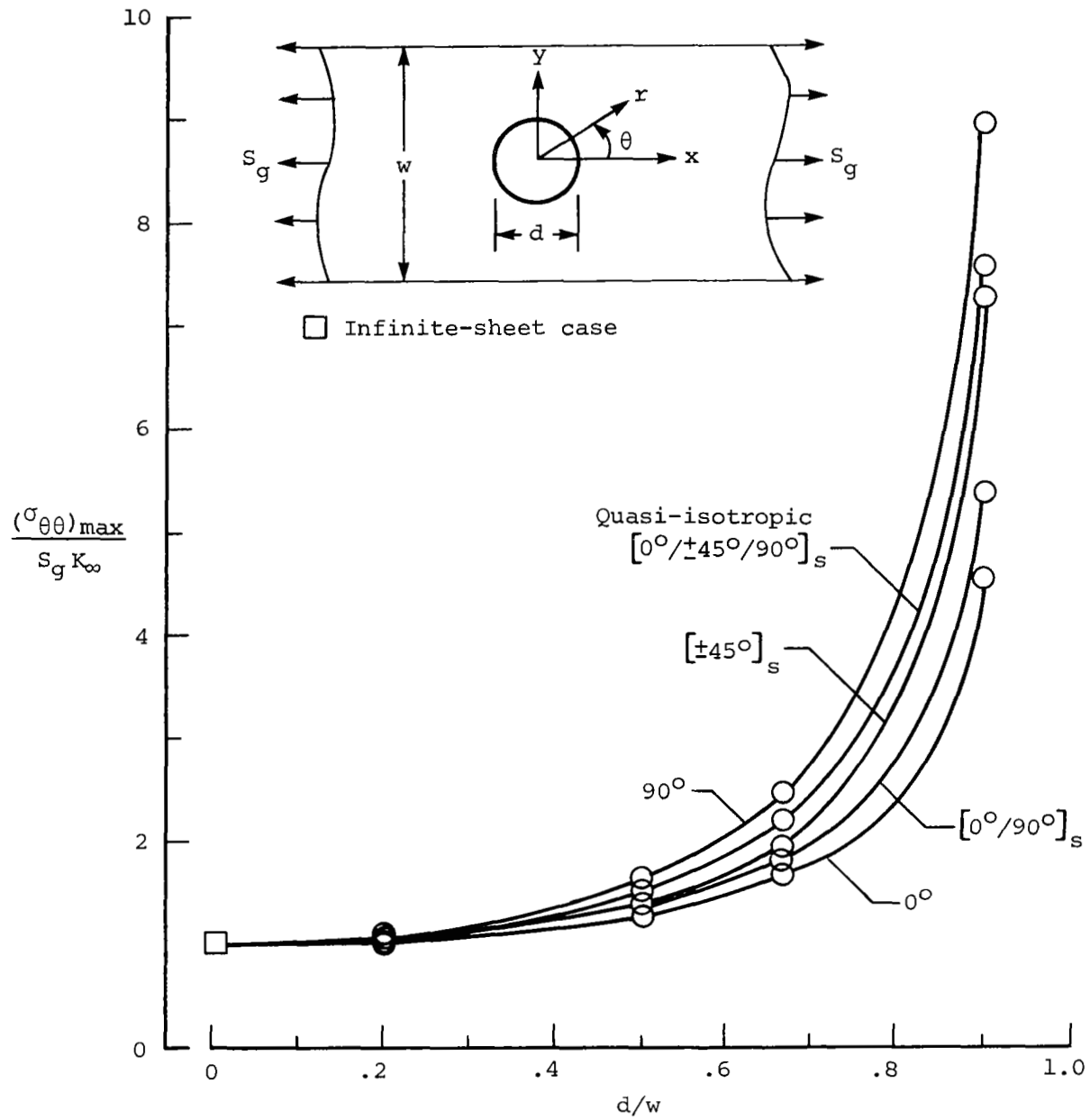

Figure 15.- Normalized maximum stress in orthotropic laminates with a circular hole and uniform stress boundary condition; L/w = 10.

1. Report No.	2. Government Accession No.	3. Recipient's Catalog No.
NASA TP-1469		

4. Title and Subtitle	5. Report Date
STRESS-CONCENTRATION FACTORS FOR FINITE ORTHOTROPIC LAMINATES WITH A CIRCULAR HOLE AND UNIAXIAL LOADING	May 1979
	6. Performing Organization Code

7. Author(s)	8. Performing Organization Report No.
C. S. Hong and John H. Crews, Jr.	L-12744
	10. Work Unit No. 506-17-23-03
9. Performing Organization Name and Address NASA Langley Research Center Hampton, VA 23665	11. Contract or Grant No.
	13. Type of Report and Period Covered Technical Paper
12. Sponsoring Agency Name and Address National Aeronautics and Space Administration Washington, DC 20546	14. Sponsoring Agency Code

15. Supplementary Notes

C. S. Hong: NRC-NASA Resident Research Associate.
John H. Crews, Jr.: Langley Research Center.

16. Abstract

Stresses were calculated for finite-width orthotropic laminates with a circular hole and remote uniaxial loading using a two-dimensional finite-element analysis with both uniform stress and uniform displacement boundary conditions. Five different laminates were analyzed: quasi-isotropic $[0^\circ/\pm45^\circ/90^\circ]_s$, 0°, 90°, $[0^\circ/90^\circ]_s$, and $[\pm45^\circ]_s$. Computed results are presented for selected combinations of hole-diameter—sheet-width ratio d/w and length-to-width ratio L/w.

For small L/w values, the stress-concentration factors K_{tn} were significantly different for the uniform stress and uniform displacement boundary conditions. Typically, for the uniform stress condition, the K_{tn} values were much larger than for the infinite-strip reference condition; however, for the uniform displacement condition, they were only slightly smaller than for this reference.

The results for long strips are also presented as width-correction factors. For $d/w \leq 0.33$, these width-correction factors are nearly equal for all five laminates.

17. Key Words (Suggested by Author(s))	18. Distribution Statement
Composites Finite-width Orthotropic Stress-concentration factor Circular hole Elastic	Unclassified - Unlimited Subject Category 24

19. Security Classif. (of this report)	20. Security Classif. (of this page)	21. No. of Pages	22. Price*
Unclassified	Unclassified	26	$4.00

*For sale by the National Technical Information Service, Springfield, Virginia 22161

NASA-Langley, 1979

National Aeronautics and Space Administration

Washington, D.C.
20546

Official Business
Penalty for Private Use, $300

THIRD-CLASS BULK RATE

Postage and Fees Paid
National Aeronautics and
Space Administration
NASA-451

U.S. MAIL

7 1 1U,C, 051179 S00903DS
DEPT OF THE AIR FORCE
AF WEAPONS LABORATORY
ATTN: TECHNICAL LIBRARY (SUL)
KIRTLAND AFB NM 87117

NASA

POSTMASTER: If Undeliverable (Section 158 Postal Manual) Do Not Return